

Impact of Velocity and Wind Direction to Drag Force of Commercial Train Locomotive

Ahmad Imam Khoiruddin^{1,a}

¹Mechanical Engineering Department, Universitas Pertamina, Jakarta, Indonesia

^aahmadimamkh@gmail.com

Abstrak.

Penelitian ini membahas analisis mengenai hubungan antara kecepatan lokomotif dan arah angin terhadap besarnya hambatan udara yang dihadapi lokomotif CC203, salah satu lokomotif tercepat yang digunakan di Indonesia saat ini. Berdasarkan hasil analisis tersebut, dibuat opsi geometri alternatif untuk moncong lokomotif CC203. Pada opsi geometri, dilakukan perubahan pada struktur depan lokomotif agar dapat mengurangi besar hambatan udara yang terjadi. Berdasarkan hasil analisis yang telah dijalankan, semakin besar kecepatan lokomotif, nilai koefisien hambatan udara akan cenderung konstan, namun nilai keseluruhan gaya hambatan udara akan semakin membesar. Selain itu, perubahan arah angin yang menghadapi lokomotif juga akan menaikkan nilai koefisien dan gaya hambatan udara secara signifikan. Pada perubahan geometri lokomotif, didapatkan hasil opsi geometri yang dapat menurunkan nilai koefisien dan gaya hambatan udara total secara signifikan. Kecepatan lokomotif diasumsikan sebagai resultan dari kecepatan angin.

Kata kunci: *depan lokomotif, koefisien drag, drag force*

Abstract.

An analysis of the relationship between locomotive speed and wind direction was carried out on the amount of drag force faced by the CC203 locomotive, one of the fastest locomotives used in Indonesia today. Based on the results of the analysis, an alternative geometry option was made for the CC203 locomotive's nose. In the geometry option, changes are made to the front structure of the locomotive in order to reduce the amount of air drag that occurs. Based on the results of the analysis that has been carried out, the greater the speed of the locomotive, the value of the drag coefficient will tends to be constant, but the overall value of the drag force will increase. In addition, changes in wind direction facing the locomotive will also significantly increase the coefficient and air drag force. In changing the locomotive geometry, the results of geometric options are obtained that can significantly reduce the coefficient and total air resistance force. Locomotive velocity was assumed as resultant of wind velocity.

Keywords: *front of the locomotive, drag coefficient, drag force*

Introduction

The train is one of the reliable modes of transportation. This mode of transportation is able to move many people from one place to another in a short time. When the train runs, like any other vehicle, there is a resistance caused by the air. This resistance causes aerodynamic forces on the vehicle. The forces that affect the interaction of air with solid objects are aerodynamic lift and aerodynamic resistance (drag) [1].

In the case of drag force, many studies have been carried out for various types of trains, such as Wulandari's research [2] which focuses on the effect of the air resistance coefficient on the aerodynamic force that occurs in the CC203 locomotive using the wind tunnel test method; research of Tolman et al. [3] and Stucki [4] who discuss the optimization of the locomotive nose design to reduce drag using the Computational Fluid Dynamics (CFD) method; Paniagua and Garcia's research

[5] which discusses the optimization of the nose design of the high-speed train to reduce the drag coefficient from the front (zero yaw-angle condition) using the CFD method; and research by Premoli et al. [6] which compared aerodynamic tests between fast moving and stationary trains using CFD simulation and validated by wind tunnel tests.

However, not many aerodynamic studies have focused on locomotives. Therefore, the author decided to examine the aerodynamic phenomena that occurred in one of the fastest locomotives in Indonesia, namely the CC203 locomotive. Analysis was carried out using the CFD method, and the results will be validated using the wind tunnel test data from Wulandari's research [2] and other researches. This locomotive has an empty weight of 78 tons, so it can overcome the lift force, and has a maximum speed of 120 km/hour [7]. With this high maximum speed, aerodynamic phenomena will definitely occur on the locomotive, so this phenomenon becomes important to study. The aerodynamic phenomena analyzed are the influence of locomotive speed and the effect of wind direction on the drag coefficient. The two results of the analysis will later become the basis for making options for changing the nose geometry of the locomotive, which is expected to reduce the drag coefficient value, thereby reducing the air resistance experienced by the locomotive. The test uses wind conditions from the front of the locomotive (zero yaw-angle condition) and the side of the locomotive (yaw angle 0-30°). The angle 0-30° was chosen because this angle is the angle where the wind comes from when the train is at high speed [6]. The locomotive speed is assumed to be the resultant of air velocity with the locomotive model when it is in a straight line with the air velocity (zero yaw angle), and not moving (velocity 0 m/s). This is adjusted to Wulandari's research [2] which will be data validation reference. The air speed is set at 25 - 29 m/s in the simulation of the forward wind direction, and 29 m/s in the simulation of the side wind direction.

Important Equation

Drag force is the resultant force in the opposite direction to the wind speed, on an object when facing a fluid flow. Meanwhile, the lift force is the resultant force that is perpendicular (normal) to the direction of fluid flow [8]. Drag and lift forces arise because of the shear stress and pressure forces that occur on the surface of the object. In the case of the CC203 locomotive, the lift force is not the focus of the study, because the mass of the CC203 locomotive reaches 78 tons, which can overcome the lift force that can occur at maximum speed.

The calculation of drag force is determined by:

$$D = \frac{1}{2} C_D \rho U^2 A \tag{1}$$

- C_D = drag coefficient
- D = drag force (N)
- ρ = air density (kg/m³)
- U = air velocity (m/s)
- A = frontal area (m²)

Reynolds Number (R_e) is the ratio between the inertial force and the viscous force that occurs in a fluid flow. Formulated as follows.

$$R_e = \frac{UL}{\nu} = \frac{\rho UL}{\mu} \tag{2}$$

- R_e = Reynolds Number
- U = air velocity (m/s)
- L = length of the locomotive (m)

ν	= kinematic viscosity (m^2/s)
μ	= dynamic viscosity (kg/ms)
ρ	= air density (kg/m^3)

CAD Modelling

The CC203 locomotive modeling is based on the locomotive dimensions listed in Wulandari's research [2]. The locomotive dimension data is based on official data from PT Kereta Api Indonesia (Persero) Daerah Operasi 6 Yogyakarta. The modeling was carried out using the Solidworks 2017 software. For the simulation, the locomotive will be modeled on a 1:70 scale, based on Wulandari's research [2] for validation purposes.

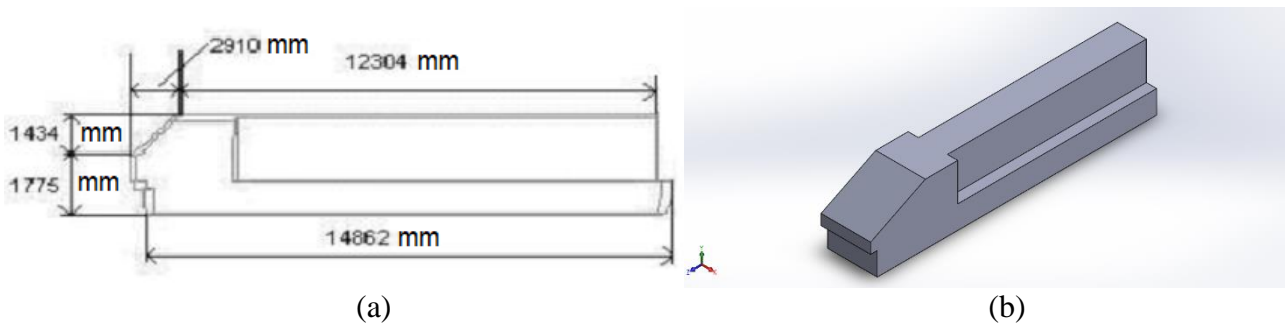


Fig. 1. (a) Dimension of CC203 locomotive [2]; (b) Modelling of CC203 locomotive

CFD Simulation Layout

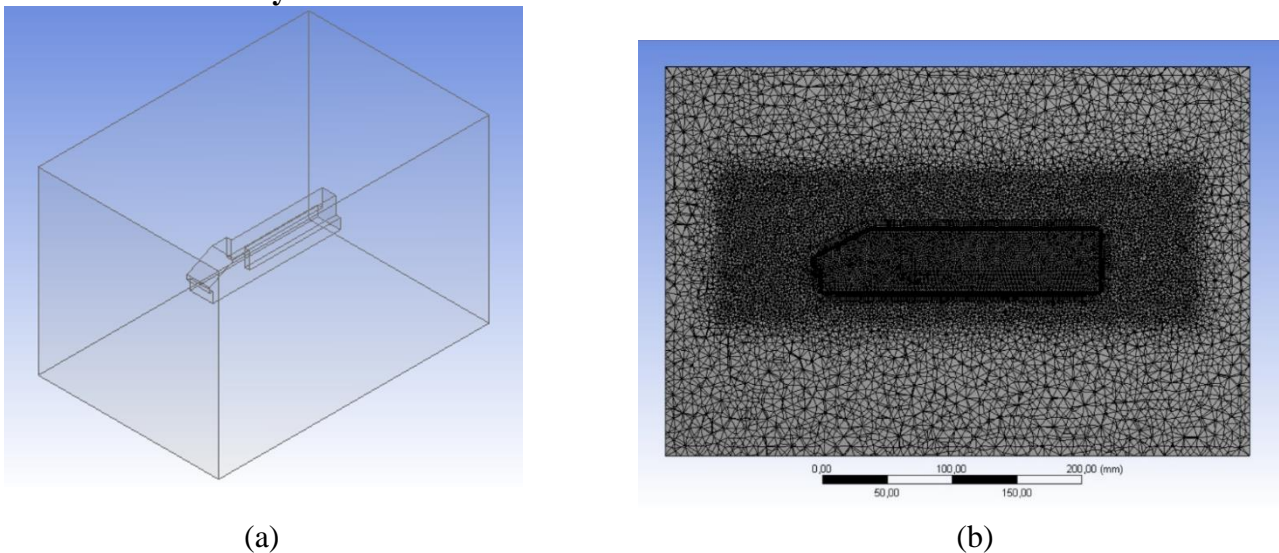


Fig. 2 (a) Modelling and enclosure used in this research; (b) Meshing

This simulation uses enclosure with size $450 \times 300 \times 300$ mm, based on Wulandari's research [2], and uses Tetrahedron mesh. This meshing mode was applied due to the shape complexity of the CC203 nose. Also, the mesh intensity around the locomotive was increased to accommodate the turbulent flow around the locomotive. Mesh Independence Study has been done, resulting in 2,586,167 elements effective to use in this simulation.

However, this CFD simulation uses SST k-omega approach, due to its reliability on fluid simulation [5].

Simulation Validation

This process is a comparison between the results of the simulation carried out against the data from the wind tunnel test available for the CC203 locomotive. As a comparison, data from Wulandari's research [2] was used which had tested the air resistance of the CC203 locomotive using a wind tunnel. The simulation treatment is the same as Wulandari's research, namely the treatment of fluid flow from the front of the locomotive (zero yaw angle) and the flow velocity range is also the same (25-29 m/s). The validation results are shown in the following graph.

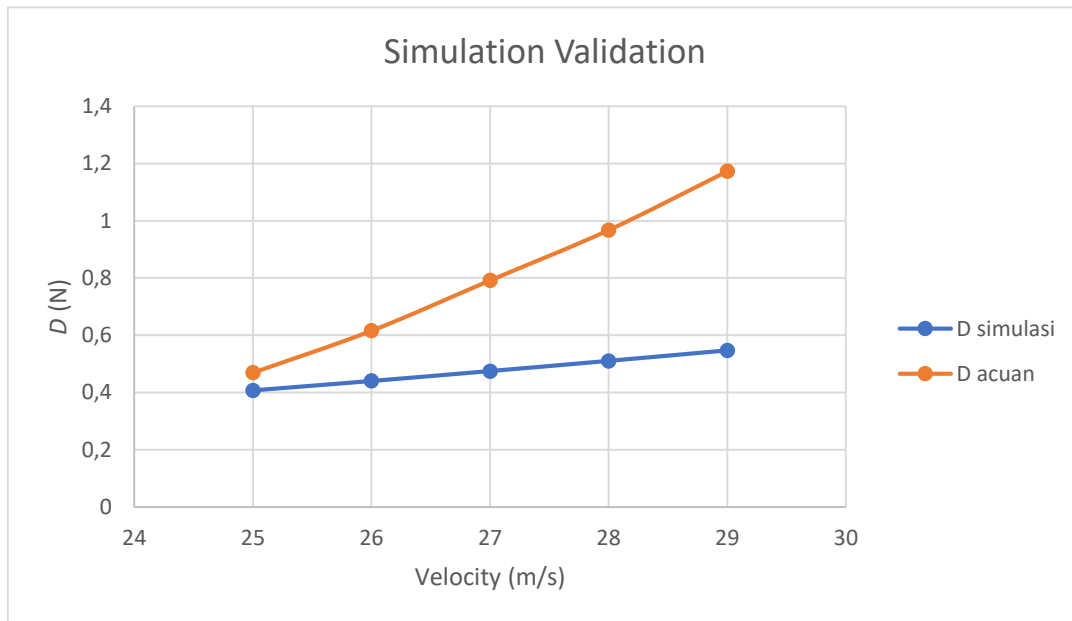


Fig. 3 Simulation Validation Graph. The “D simulasi“ is for CFD simulation results, and “D acuan“ is for Wulandari’s research results [2]

There is an increasing difference (error) between the D value from the simulation results and the results of the Wulandari wind tunnel experiment [2], along with the increase in fluid velocity. Based on direct interviews with the researcher of this study, the difference is caused by the surface of the Wulandari locomotive specimen using wood material, so it greatly affects the magnitude of the test results, considering the roughness of the wood is greater than the aluminum material used in the C_D simulation. In addition, it is suspected that there was an error in the manufacture of the specimen, so that the size of the specimen did not match the required size, thus affecting the results of the study.

Meanwhile, in the simulation of train air resistance which uses aluminum material and has a locomotive muzzle shape that is almost the same, the test results show that the C_D value is not much different from the C_D simulation results. The comparison is shown in the following table [9].

Table 1 Comparison of C_D Value between Trains

No.	Train	Experiment Method	C_D	C_D of CC203 ($v = 29$ m/s)	% err
1	ICE 1 (Germany)	Coasting	0.72	0,67094744	-7.31

2	TGV 001 (France)	Coasting	0.65	0,67094744	3.12
3	KTX (Korea)	Coasting	0.73	0,67094744	-8.8

Based on the comparison in Table 1, it can be seen that in the C_D simulation results with the results of the train aerodynamics test with a similar muzzle shape, there is no significant difference in the C_D value. The highest difference between the CC203 locomotive CFD simulation results and the experimental results of the three train examples above only reached 8.8% on the KTX train. So, with that percentage of the difference, according to the research of Yulianto et al. [10], it can be concluded that the C_D simulation carried out is valid or in accordance with the conditions in the field.

CFD Simulation of CC203 Locomotive

The results of the simulation of changes in wind speed and wind direction are shown in the following graph.

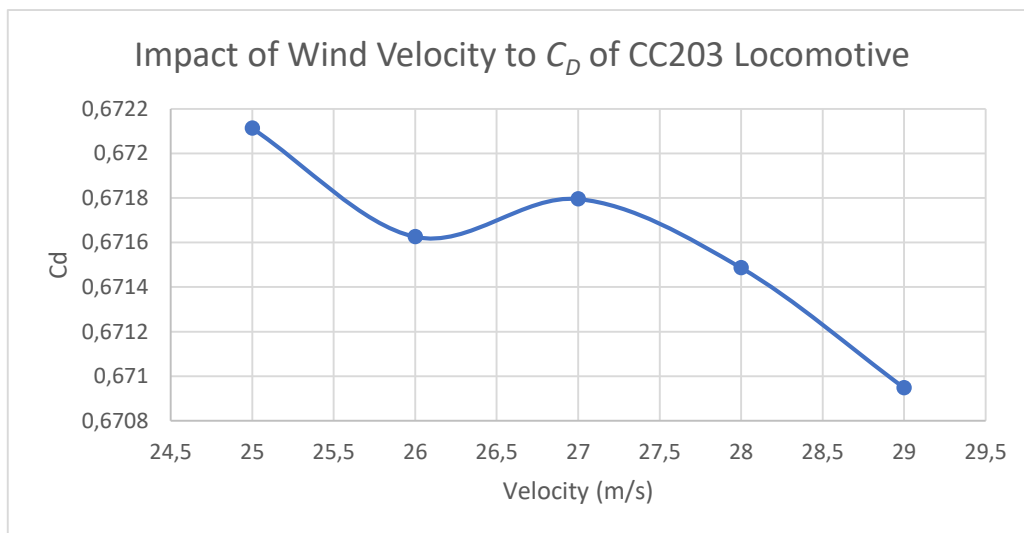


Fig. 4 Graph of Changes in Wind Velocity against C_D Value of CC203 Locomotive

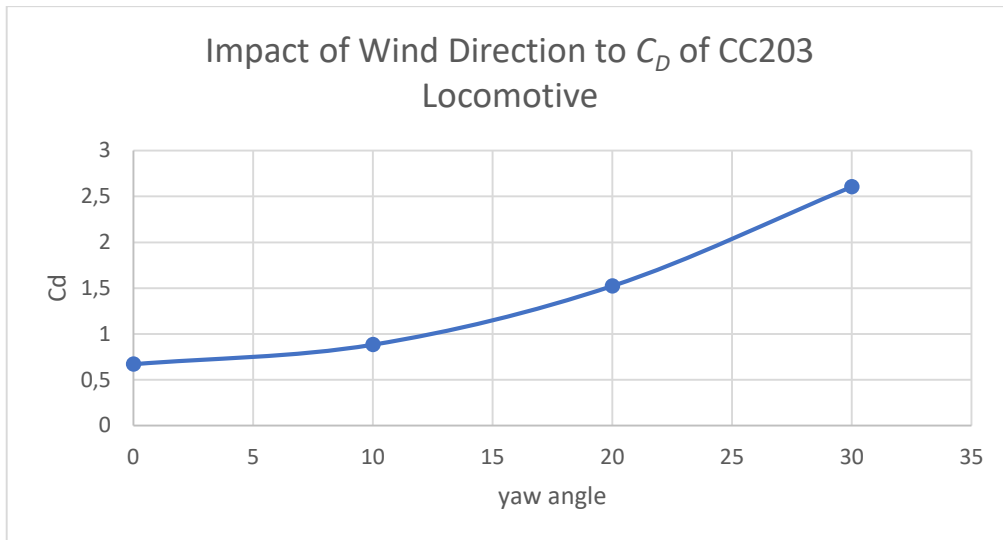


Fig. 5 Graph of Changes in Wind Direction against C_D Value of CC203 Locomotive

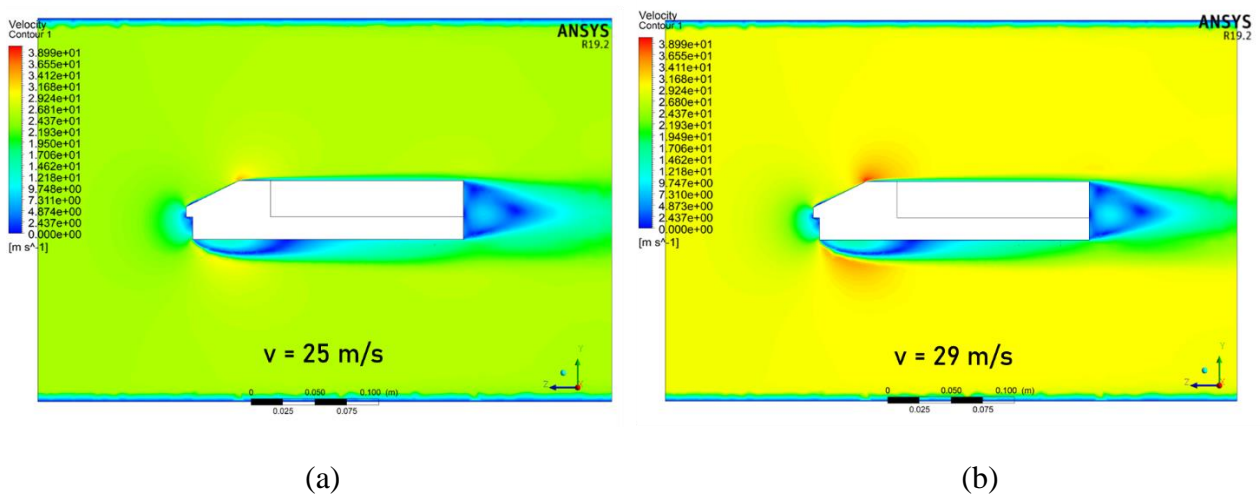


Fig. 6 Velocity Contour around the locomotive in the wind velocity (a) 25 m/s, and (b) 29 m/s. Seen, the turbulence of the flow is concentrated at the corners of the muzzle of the locomotive, and the turbulence is increasing as the velocity increases.

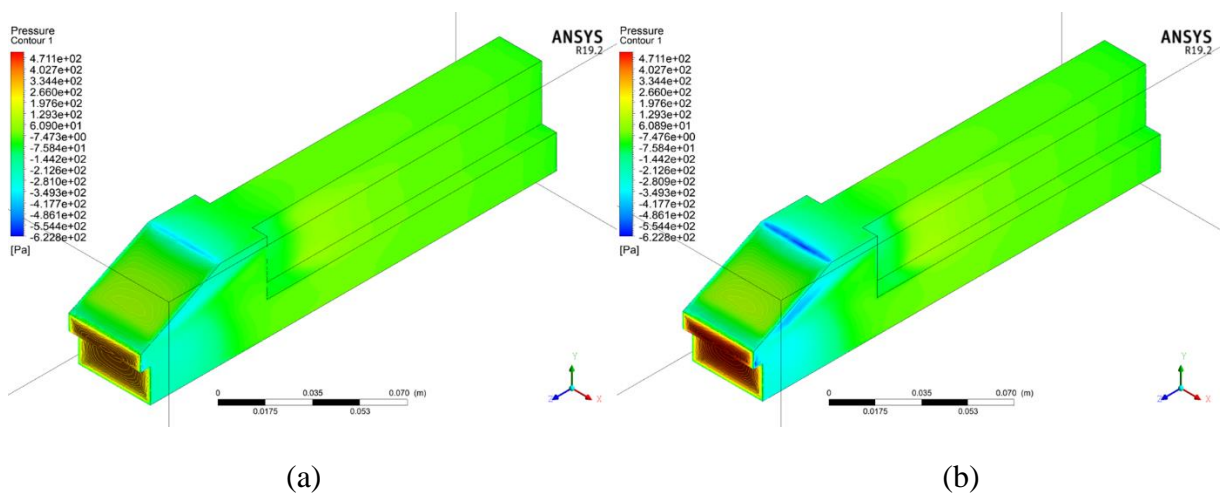


Fig. 7 Pressure Contour in locomotive body in the wind velocity (a) 25 m/s, and (b) 29 m/s. Seen, the pressure is increasing as the velocity increase.

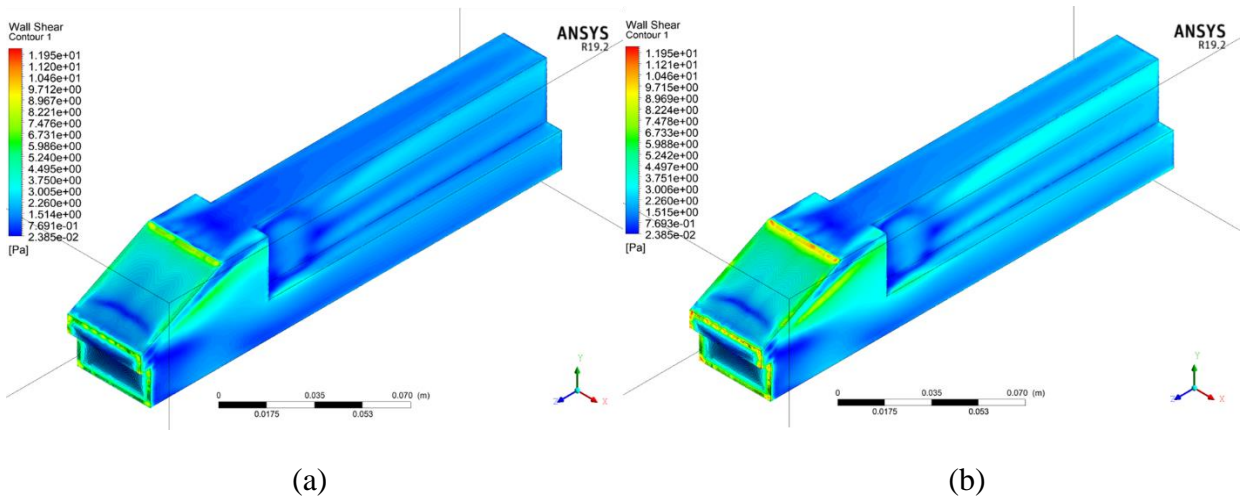


Fig. 8 Shear Stress Contour in locomotive body in the wind velocity (a) 25 m/s, and (b) 29 m/s. Seen, the shear stress is increasing as the velocity increase.

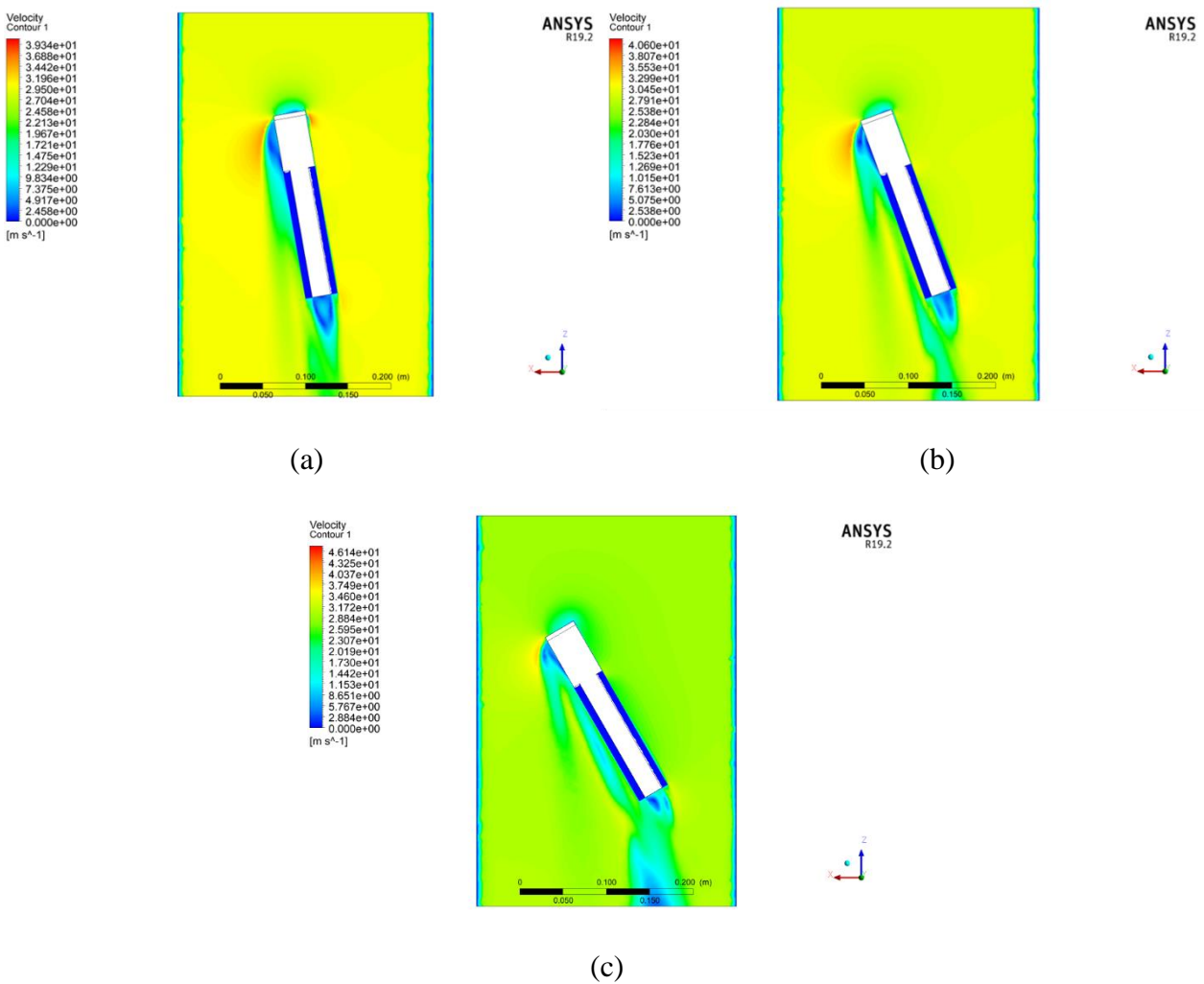


Fig. 9 Velocity contour of yaw angle: (a) 10^0 , (b) 20^0 , dan (c) 30^0

Based on the simulation results, it can be seen that as the locomotive speed increases, the C_D value will tend to fluctuate in a very close range. It can be seen that the difference between the highest and lowest C_D values in this simulation (0.67211311 and 0.67094744) is only 0.17%, so it can be said that the C_D values in this simulation are constant. This is due to a property, that in fluid flow that moves facing a blunt body, the value of C_D will tend to be constant over a certain range of Re numbers [8]. In this simulation, the C_D value is constant in the range of Re 3.4×10^5 (at a speed of 25 m/s) to 3.9×10^5 (at a speed of 29 m/s). Similar results were also shown by the research of Schewe [11] which showed that, in the fluid flow experiment facing a trapezoidal body, the value of C_D will be constant at the value of Re above 1×10^5 . Although the value of C_D is constant, the overall value of air resistance (D) keep moving up. The increase in the value of the air resistance force is due to an increase in pressure and friction (shear stress) that occurs in the locomotive body along with the increase in locomotive speed, resulting in an increase in the value of the air resistance force which is influenced by these two factors. In addition, mathematically, referring to Equation 1, it can be seen that the variables that affect the magnitude of D are C_D , density (ρ), wind speed (U), and locomotive cross-sectional area (A). In this case, the variables and A are set constant, and the variable C_D is also constant from the simulation results. So, the increase in the value of the locomotive drag force is mainly caused by the increase in the value of the air velocity (U). So, it can be concluded that the greater the locomotive speed, the greater the overall air resistance experienced by the locomotive.

In addition, it is also seen that the greater the yaw angle, the greater the value of C_D . This is due to the wider fluid flow separation, due to the turning of the locomotive at an angle of 0 to 30° . It can be seen in Figures 9 a to c, the separation the flow becomes wider as the yaw angle increases, so the flow becomes more turbulent, and increases the air resistance experienced by the locomotive.

Geometry Options

Based on the simulation of changes in wind speed and wind direction that have been carried out previously, it can be seen that the locomotive body receives the largest wind pressure force on the front-bottom (cowcatcher section, locomotive wheel barrier) and receives the largest wind friction force on the front-upper side (obtuse angle at the top). the top of the locomotive) and the front-side (the angle between the front and side of the locomotive body) (see Figures 7-8). Therefore, a geometric option was made that modifies these parts, in order to minimize the pressure and friction values optimally, so that in the end it can minimize the air resistance that faces the locomotive. The locomotive geometry options are made using the heuristic-intuitive method, based on the pressure and friction contours of the previous simulation results.

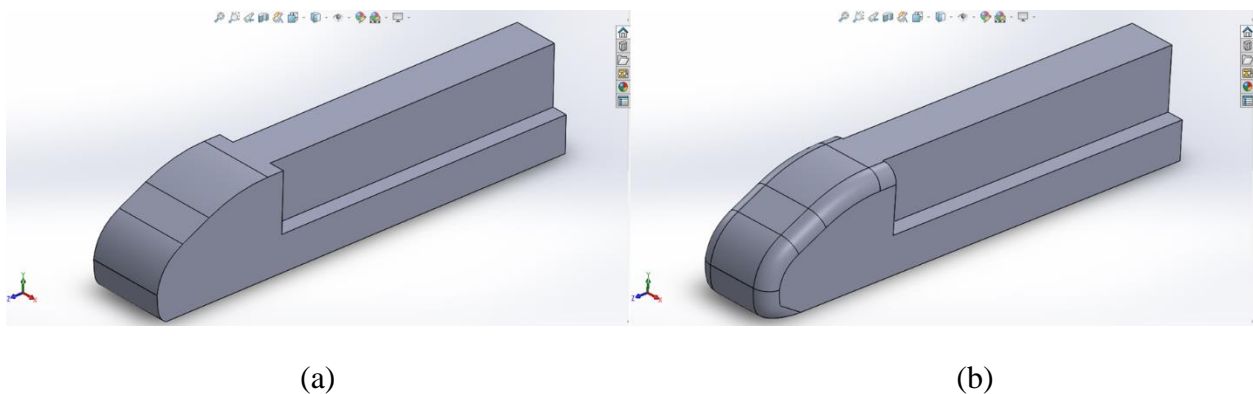


Fig. 10 Geometry Options (a) 1; (b) 2

CFD Simulation of Geometry Options

The results of the simulation of changes in wind speed and wind direction for locomotive geometry options are shown in the following graphs.

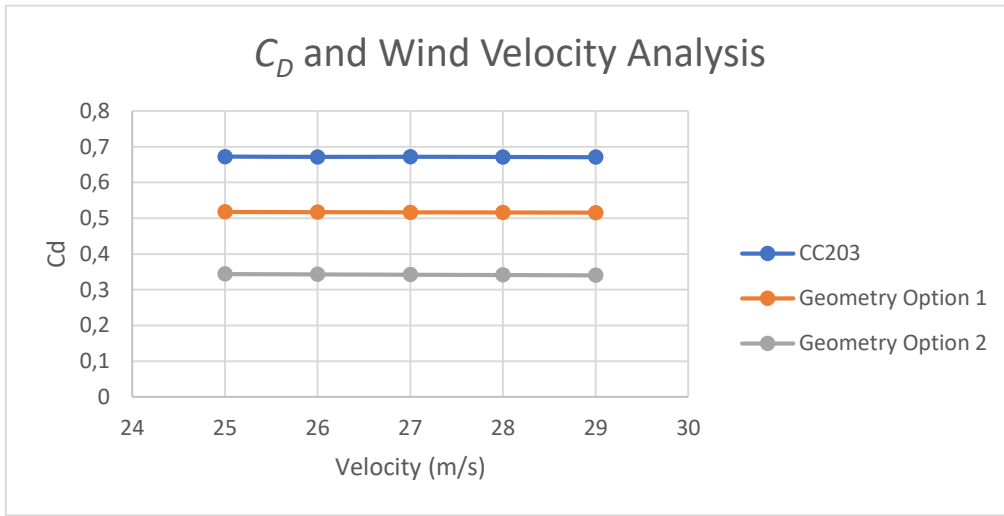


Fig. 11 Graph of Comparison of Changes in Wind Velocity to C_D Value in the three locomotive nose designs

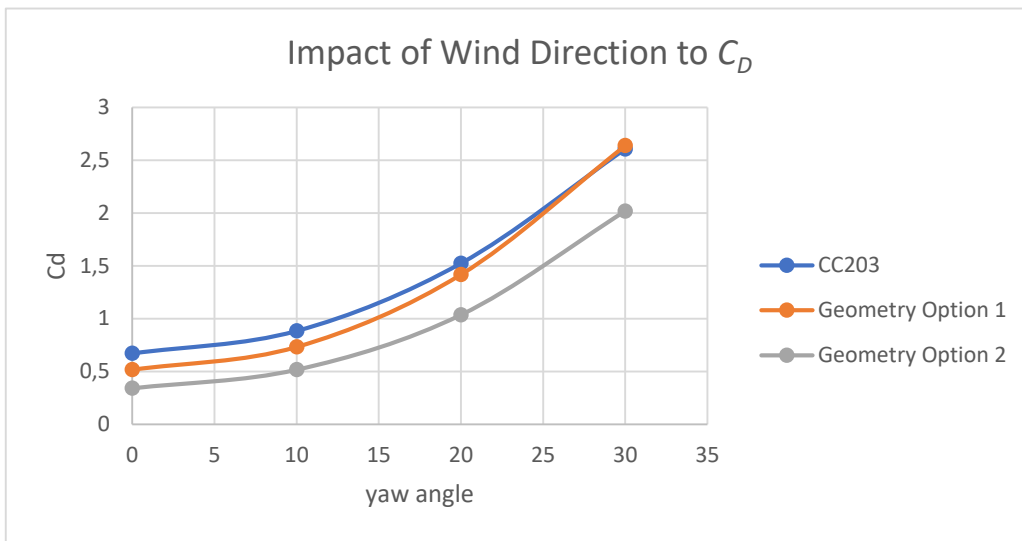
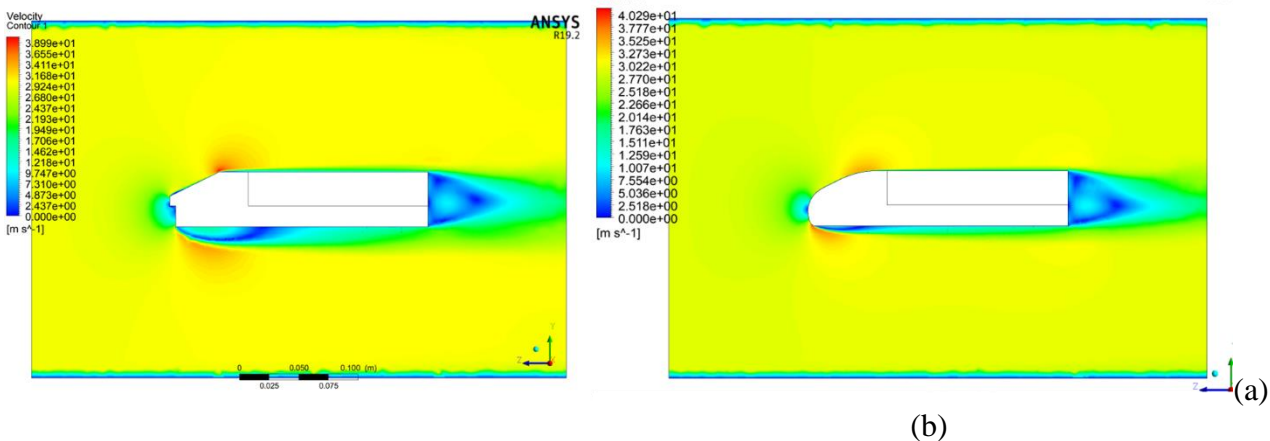
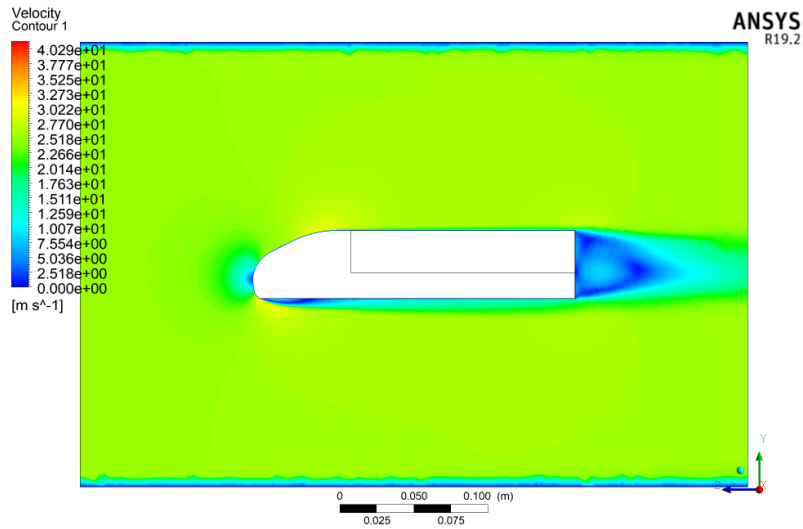


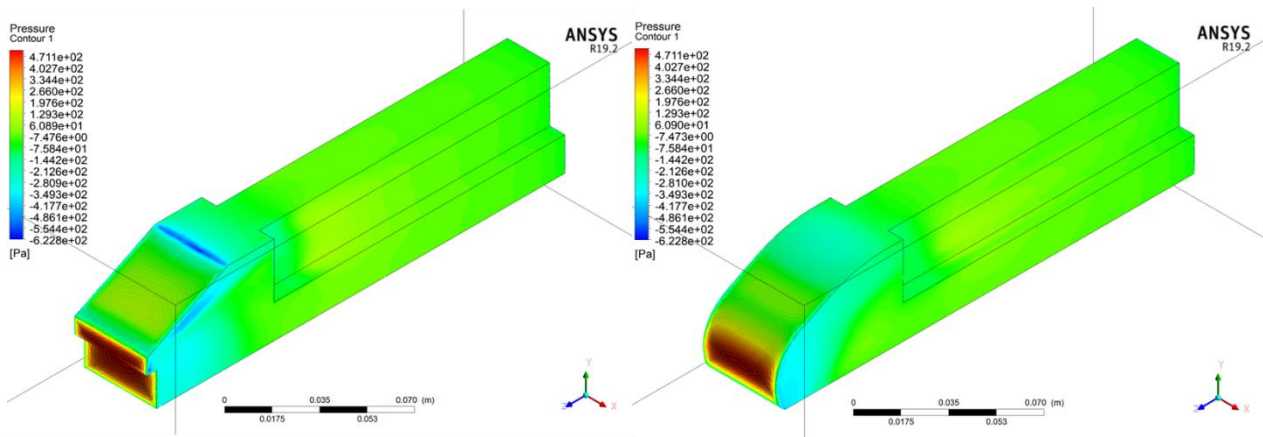
Fig. 12 Graph of Comparison of Changes in Wind Direction to C_D Value





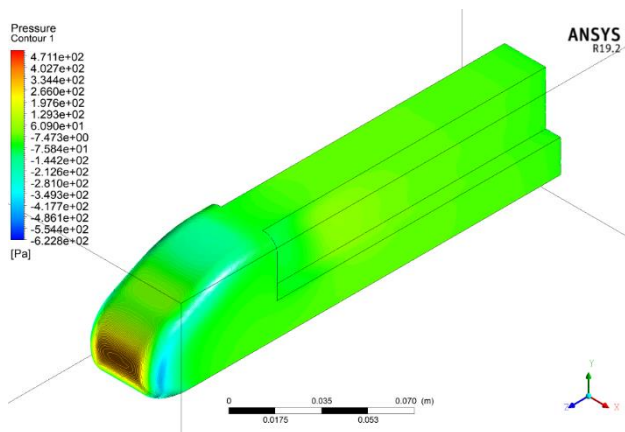
(c)

Fig. 13 Velocity Contour around the locomotive in the Geometry Options (a) CC203; (b) 1; and (c) 2 at velocity 29 m/s. Seen, the turbulence of the flow is decreased as the design change.



(a)

(b)



(c)

Fig. 14 Pressure Contour in locomotive body in the Geometry Options (a) CC203; (b) 1; and (c) 2 at velocity 29 m/s. Seen, the pressure is decreasing as the design change.

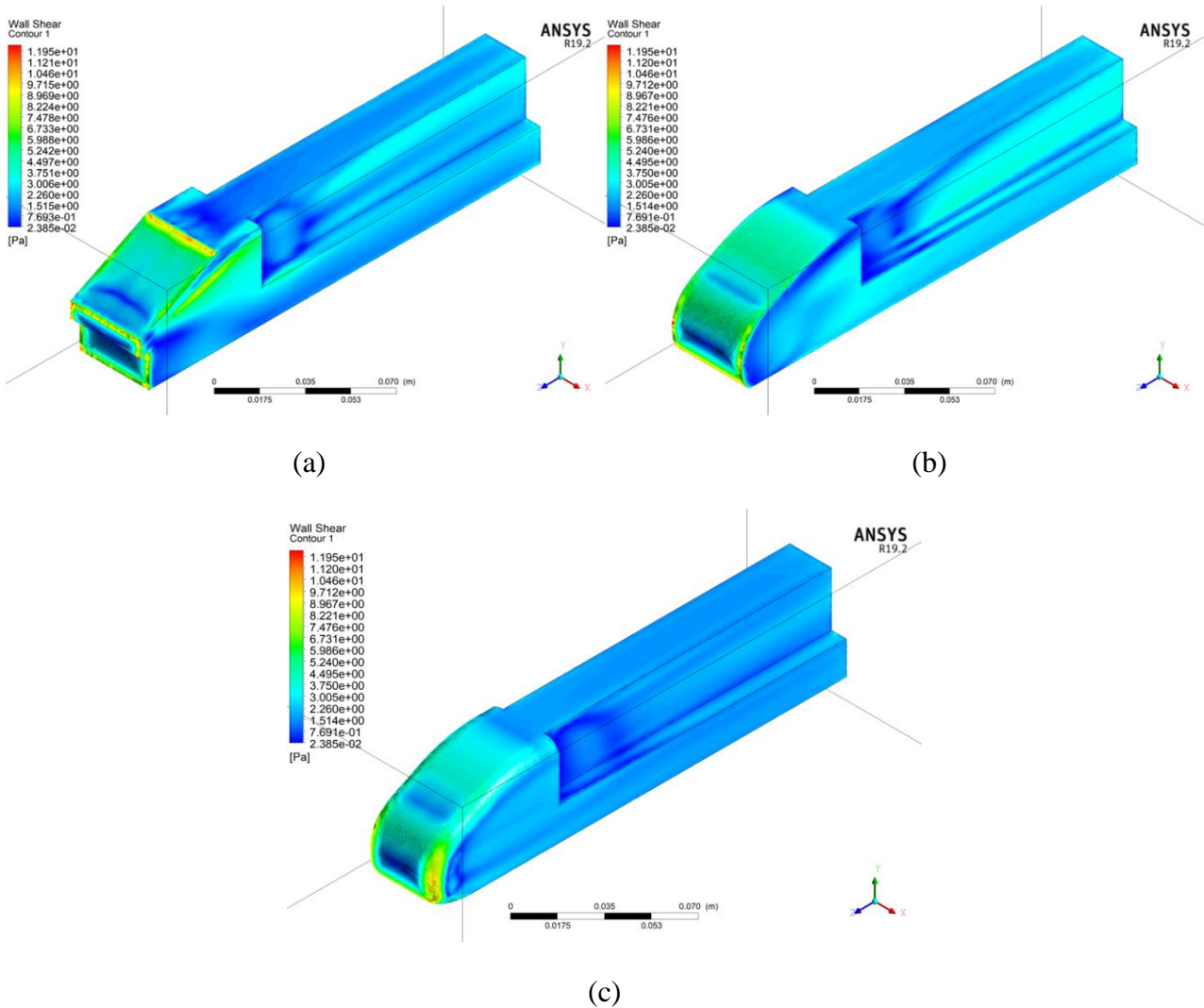


Fig. 15 Shear Stress Contour in locomotive body in the Geometry Options (a) CC203; (b) 1; and (c) 2 at velocity 29 m/s. Seen, the shear stress is decreasing as the design change.

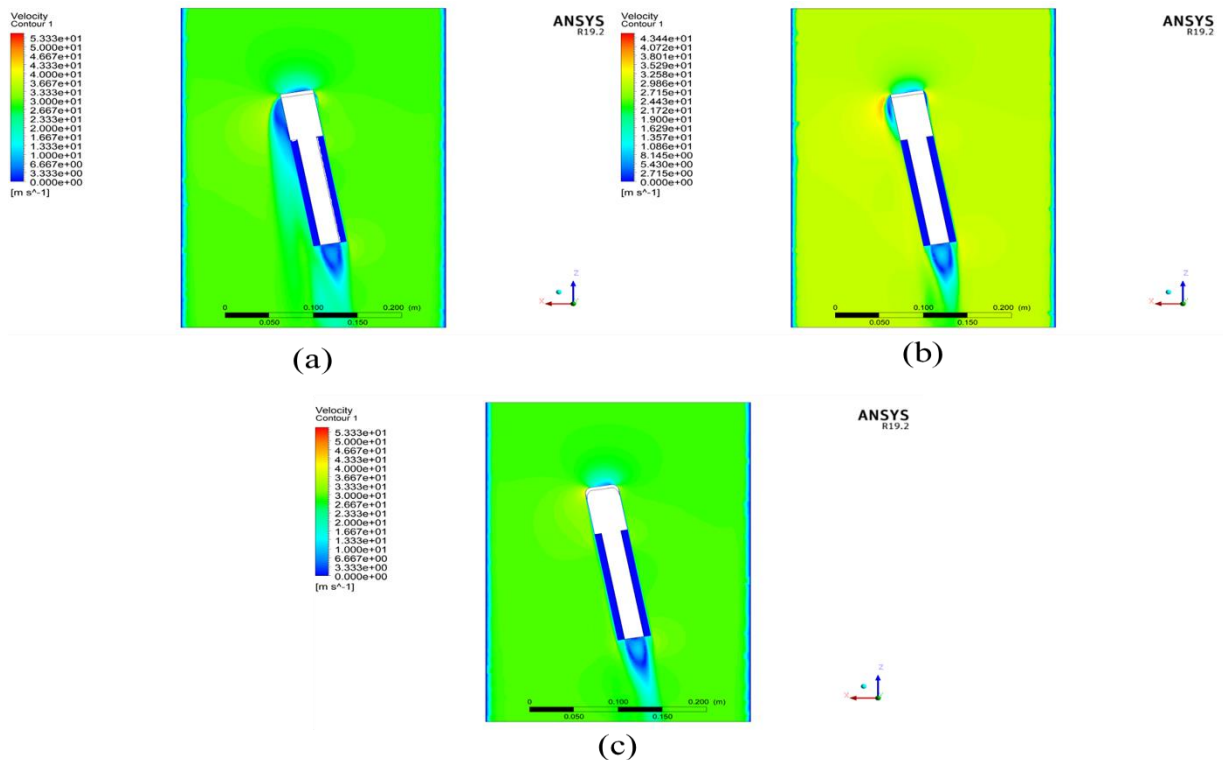


Fig. 16 Velocity Contour around the locomotive at 10^0 yaw angle in the Geometry Options (a) CC203; (b) 1; and (c) 2 at velocity 29 m/s. Seen, the turbulence of the flow is decreased as the design change.

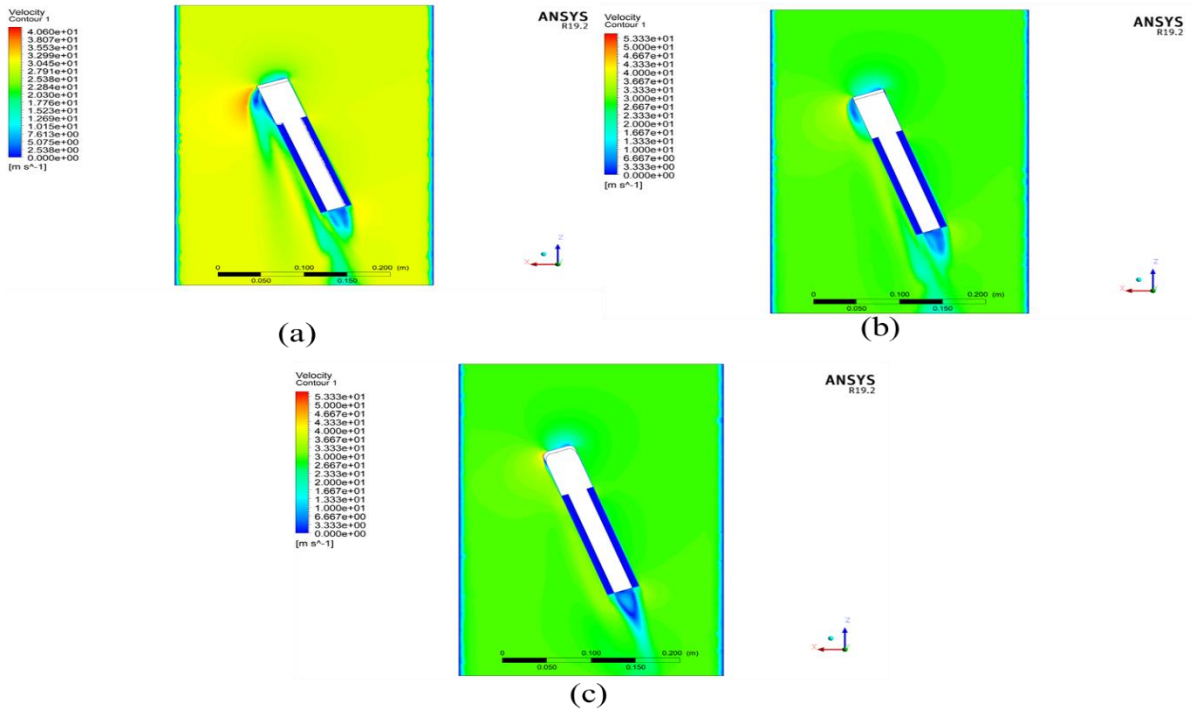


Fig. 17 Velocity Contour around the locomotive at 20^0 yaw angle in the Geometry Options (a) CC203; (b) 1; and (c) 2 at velocity 29 m/s. Seen, the turbulence of the flow is decreased as the design change.

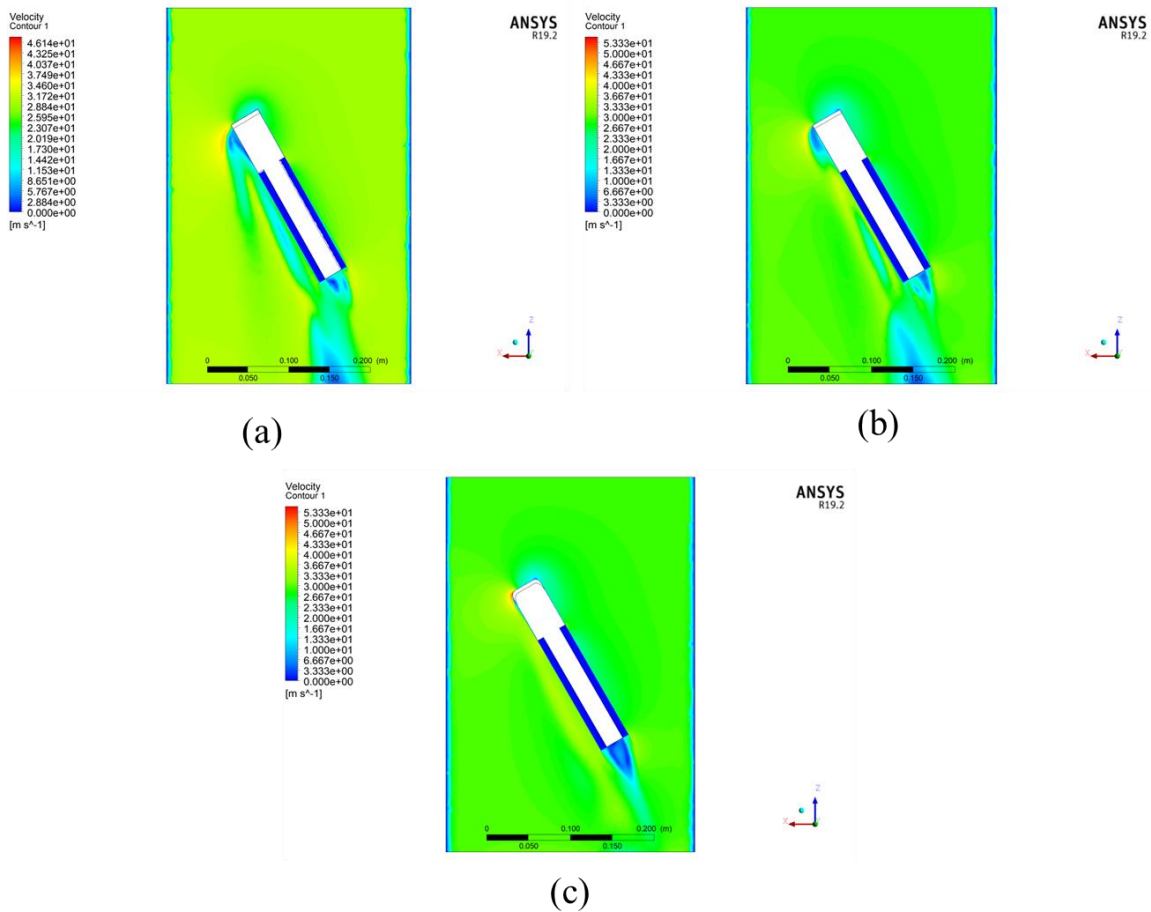


Fig. 18 Velocity Contour around the locomotive at 30^0 yaw angle in the Geometry Options (a) CC203; (b) 1; and (c) 2 at velocity 29 m/s. Seen, the turbulence of the flow is decreased as the design change.

Based on the simulation results, as in the CFD simulation for the original locomotive design, it can be seen that as the locomotive speed increases, the C_D value will tend to fluctuate in a very close range. It can be seen that the difference between the highest and lowest C_D values in the simulation of geometry option 1 (0.51776631 and 0.51565237) is only 0.41%, and in the simulation of geometry option 2 (0.3439524 and 0.3403198) it is only 1.06%. So, it can be said that the C_D values in this simulation are constant. This is due to a property, that in fluid flow that moves facing a blunt body, the value of C_D will tend to be constant over a certain range of Re numbers. For example, in fluid flow facing a sphere, the value of C_D will be constant in the range $10^3 < Re < 10^5$ [18]. Although the value of C_D is constant, the overall value of the air resistance (D) continues to move up. The increase in the value of the air resistance force is due to an increase in pressure and friction (shear stress) that occurs in the locomotive body along with the increase in locomotive speed, resulting in an increase in the value of the air resistance force which is influenced by these two factors. In addition, mathematically, referring to Equation 1, it can be seen that the variables that affect the magnitude of D are C_D , density (ρ), wind speed (U), and locomotive cross-sectional area (A). In this case, the variables and A are set constant, and the variable C_D is also constant from the simulation results. So, the increase in the value of the locomotive drag force is mainly caused by the increase in the value of the air velocity (U). So, it can be concluded that the greater the locomotive speed, the greater the overall air resistance experienced by the locomotive. In Figures 11, it can be seen that the geometry option 2 can reduce the C_D value significantly, so it can be concluded that the geometry option 2 is better than the other geometry options.

In addition, it is also seen that the greater the yaw angle, the greater the C_D and D values. This is due to the wider fluid flow separation, due to the locomotive turning at an angle of 0^0 to 30^0 . It can be seen in Figures 16 - 18. The flow separation becomes wider as the yaw angle increases, so that the flow becomes more turbulent, and increases the air resistance experienced by the locomotive. In addition, as can be seen in these images, the flow separation in geometry option 2 is smoother than the other geometry options due to the round feature at the corners of the locomotive in design 3. This also reduces flow turbulence, thereby reducing the air resistance experienced. locomotive.

Based on this explanation, it can be concluded that the geometry option that is better than other geometry options in this study to be used in an effort to reduce air resistance on the CC203 locomotive is geometry option 2, which smooths the fluid flow separation. Thus, the round feature can reduce the air resistance faced by the locomotive. It was noted that the geometry option 2 succeeded in reducing the C_D value by 49.2% at a wind speed of 29 m/s and 48.8% at a wind speed of 25 m/s.

Conclusion

Based on the simulations that have been carried out on the original CC203 locomotive model and geometry options, it can be seen that as the locomotive speed increases, the C_D value will tend to be constant. This is due to a property, that in fluid flow that moves facing a blunt body, the value of C_D will tend to be constant over a certain range of Re numbers. Although the value of C_D is constant, the overall value of the air resistance (D) continues to move up. The increase in the value of the air resistance force is due to an increase in pressure and friction (shear stress) that occurs in the locomotive body along with the increase in locomotive speed, resulting in an increase in the value of the air resistance force which is influenced by these two factors. In addition, mathematically, referring to Equation 1, it can be seen that the variables that affect the magnitude of D are C_D , density (ρ), wind speed (U), and locomotive cross-sectional area (A). In this case, the variables, A , and C_D are constant. Thus, the increase in the value of the locomotive resistance force

is mainly caused by the enlargement of the air velocity (U) value. So, it can be concluded that the greater the locomotive speed, the greater the overall air resistance experienced by the locomotive.

Afterwards, based on the simulations that have been carried out on the original CC203 locomotive model and geometry options, it can be concluded that the greater the yaw angle, the greater the C_D and D values. This is due to the wider fluid flow separation, due to the turn of the locomotive at an angle of 0° to 30° .

Then, based on the simulation that has been done, it can be concluded that the change in the geometry of the locomotive muzzle will significantly reduce the drag coefficient value. It was noted that the geometry option 2 was better than the other geometry options in reducing the drag coefficient value, and succeeded in reducing the drag coefficient value by 49.2% at a wind speed of 29 m/s and 48.8% at a wind speed of 25 m/s. This simulation also shows the importance of the round feature in designing an aerodynamic muzzle of a locomotive, because it can smooth the segregation of fluid flow. Further research can be directed at the energy efficiency that can be achieved on the CC203 locomotive if a geometry change is made that can result in a maximum reduction in air resistance.

REFERENCES

- [1] A. E. Tantowi, "Laporan Penelitian. Menentukan Matra Spoiler pada Kendaraan Minibus untuk Mempertinggi Traksi," Universitas Gadjah Mada, Yogyakarta, 1989.
- [2] B. Wulandari, "Pengaruh Koefisien Hambatan Udara pada Bentuk Lokomotif terhadap Gaya Aerodinamis Kereta Api Argo Lawu," SKRIPSI S1 Universitas Sebelas Maret, pp. 1-65, 2010.
- [3] K. Tolman, E. Crampton, C. Stucki, D. Maynes dan L. L. Howell, "Design of an Origami-Inspired Deployable Aerodynamic Locomotive Fairing," Proceedings of the 7th International Meeting on Origami in Science, Mathematics and Education, Oxford, UK, vol. 3, pp. 669-684, 2018.
- [4] C. L. Stucki, "Aerodynamic Design Optimization of a Locomotive Nose Fairing for Reducing Drag," Master Thesis of Brigham Young University, pp. 1-139, 2019.
- [5] J. M. Paniagua dan J. Garcia, "Aerodynamic drag optimization of a high-speed train," Journal of Wind Engineering & Industrial Aerodynamics, vol. 2020, no. 204, pp. 1-15, 2020.
- [6] A. Premoli, D. Rocchi, P. Schito dan G. Tomasini, "Comparison between steady and moving railway vehicles subjected to crosswind by CFD analysis," Journal of Wind Engineering and Industrial Aerodynamics, vol. 2016, no. 156, pp. 29-40, 2016.
- [7] Hartono, Lokomotif dan Kereta Diesel di Indonesia – edisi 3, Depok: Ilalang Sakti Komunikasi, 2012.
- [8] P. Gerhart, A. Gerhart and J. Hochstein, Munson, Young, and Okiishi's Fundamentals of Fluid Mechanics, New York: John Wiley & Sons, 2016.
- [9] C. Baker and T. Johnson, Train Aerodynamics: Fundamental and Applications, Oxford: Butterworth-Heinemann, 2019.

[10] A. Yulianto, K. Suastika and A. Sulisetyono, "Viscous-Resistance Calculation and Verification of Remotely Operated Inspection Submarine," IPTEK, Journal of Proceeding Series, vol. 1, pp. 26-30, 2014.

[11] G. Schewe, "Reynolds-number effects in flow around more-or-less bluff bodies," Journal of Wind Engineering and Industrial Aerodynamics, vol. 89, pp. 1267-1289, 2001.